Electronic Supplementary Material (ESI) for Nanoscale.
This journal is © The Royal Society of Chemistry 2020

SUPPLIMENTARY INFORMATION

FOR

Preparation of shape-specific (trilateral and quadrilateral) carbon quantum dots towards multiple color emission

Md Moniruzzaman [a], Buddolla Anantha Lakshmi [b], Sanghyo Kim [b] and Jongsung Kim [a, *]

[a] Department of Chemical and Biological Engineering, Gachon University, Seongnam 1342, Seongnam-daero, Seongnam-si, Gyeonggi-do 13120, Republic of Korea

[b] Department of Bionanotechnology, Gachon University, Seongnam-Si, Gyeonggi-Do 13120, Republic of Korea

∗ Corresponding author.

E-mail address: jongkim@gachon.ac.kr (J. Kim)

Table of Contents

Chemicals

Phloroglucinol, i.e., ($C_7H_6O_4$); sulfuric acid (H_2SO_4); acetone; tetrahydrofuran (THF); acetonitrile (CH_3CN); N, N-dimethylformamide (DMF); dimethylsulfoxide (DMSO); ethanol; ethyl acetate and quinine sulfate were purchased from Sigma–Aldrich, USA. All chemical reagents were used without further purification. Human cervical cancer cell line (HeLa) were acquired from CEFO Ltd, South Korea. Pencillin-streptmycin, Dulbecco's modified eagle's medium (DMEM), Trypsin-EDTA were obtained from Gibco laboratories, South Korea. Fetal bovine serum, 3-(4,5-dimethylthiazol-2-yl)-2,5-diphenyltetrazolium bromide (MTT) assay kit, Live/Dead ™ viability/cytotoxicity cell staining kit were purchased from Thermofisher scientific, USA. Deionized (DI) water was used throughout experiments and the synthesis process.

Instrumentations

PL spectrometer (Quanta Master, Photon Technology International, NJ, USA) instrument was used to record PL spectra. UV–Vis spectrophotometer (Varian Cary 100) instrument was used to measure ultraviolet–visible (UV–vis) absorption spectra. Microscope (JEM 3010, JEOL Ltd., Japan) instrument measured High-resolution transmission electron microscopy (HR-TEM) images of the as-prepared B-, G-, and Y- CQDs. FT-IR spectrometer (Bruker Vertex 70) measured Fourier transform infrared (FT-IR) spectra. X-ray photoelectron spectroscopy (XPS) was performed using an X-ray source with a twin-anode (Al-Kα, hν = 1486.6 eV) gun and a monochromatic gun. X-ray diffraction (XRD) spectra were collected using a Smart-Lab instrument (Rigaku) with a 4-kW X-ray generator and a D/teX Ultra 250 detector. Raman spectra were recorded via micro-Raman spectroscopy (ANDOR Monora500i, 633 nm).

Fluorescence lifetime decay curves were recorded using an EasyLife II fluorometer system (Photon Technology International), with auto-adjustable excitation wavelengths ranging from 260 to 650 nm. The curve fitting data were obtained using the EasyLife II program via a serial RS232 and USB connection. Fluorescence Cell imaging and in-vivo zebra fish imaging study was performed by NIKON live cell capture system.

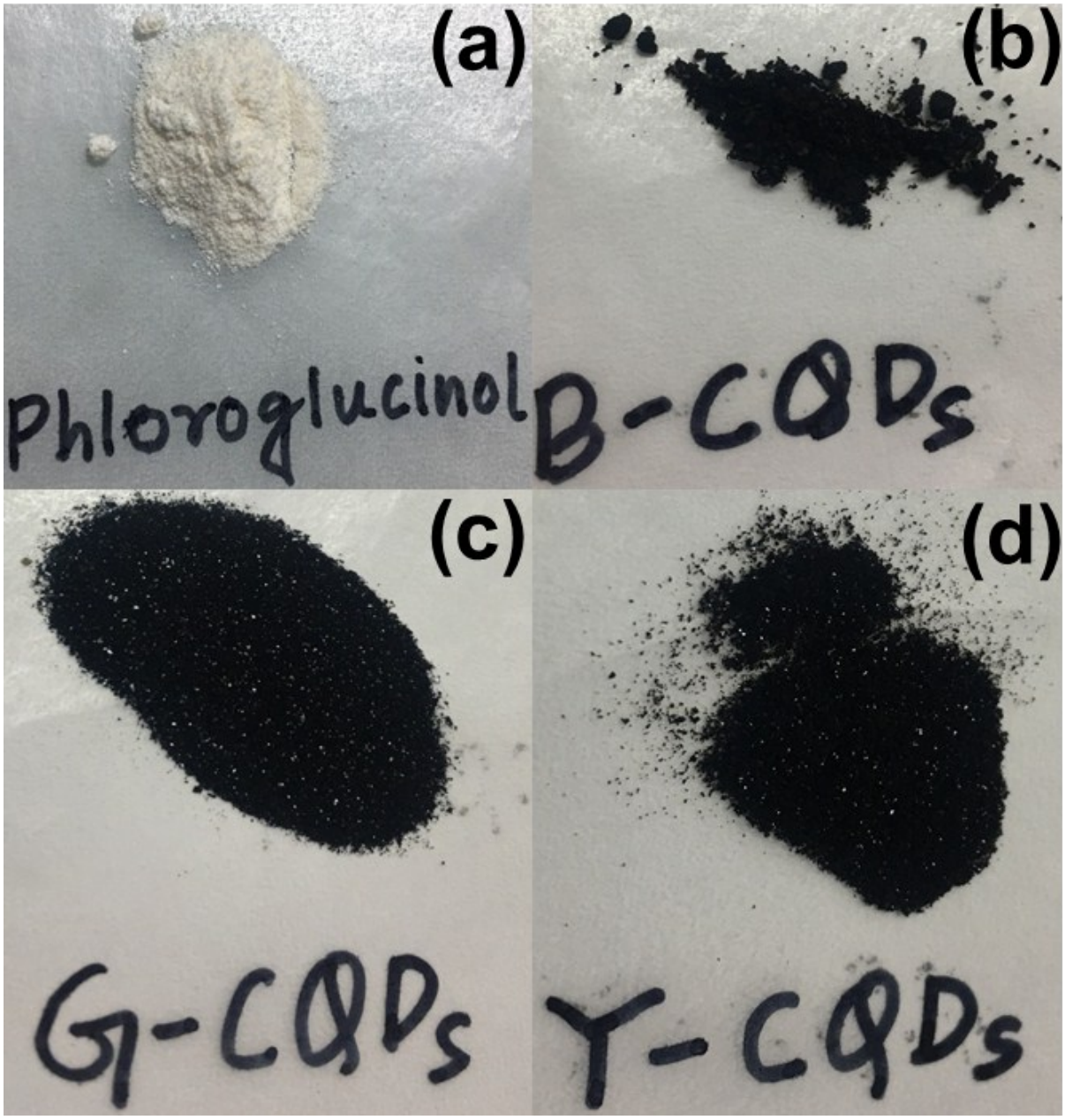

Fig. S1. Digital photographic images of (a) phloroglucinol (b) B-CQDs (c) G-CQDs (d) Y-

CQDs

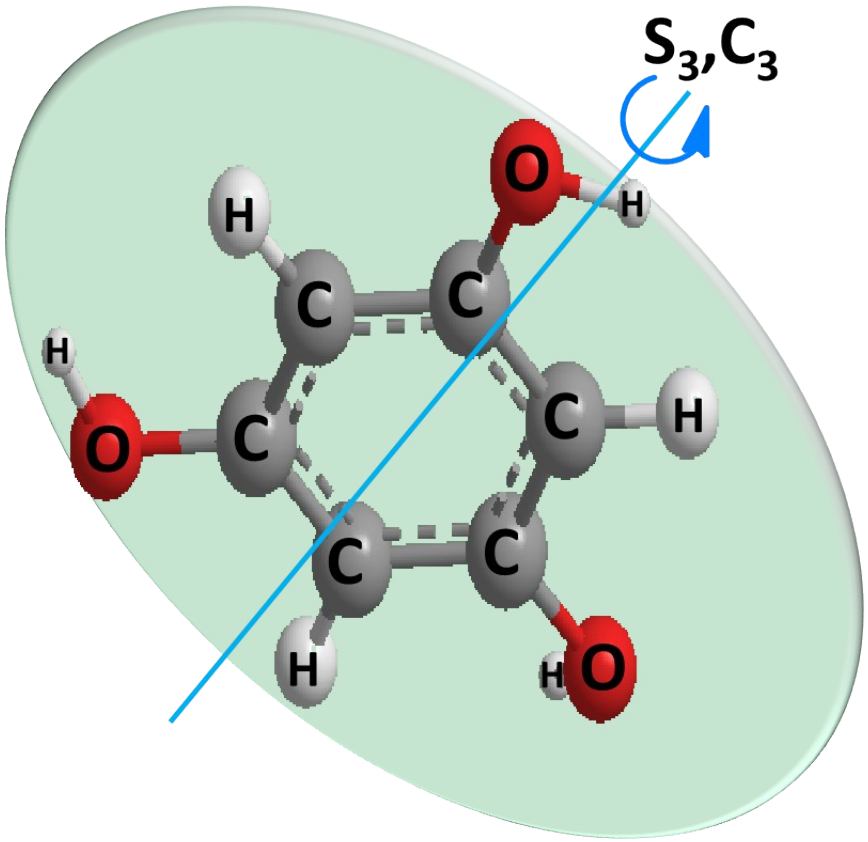

Three-fold symmetry, C_3h; symmetry elements: E, C_3, C_3^2, σ^h, S^3, S_3^{-1}

Fig. S2. Structure and symmetry of phloroglucinol

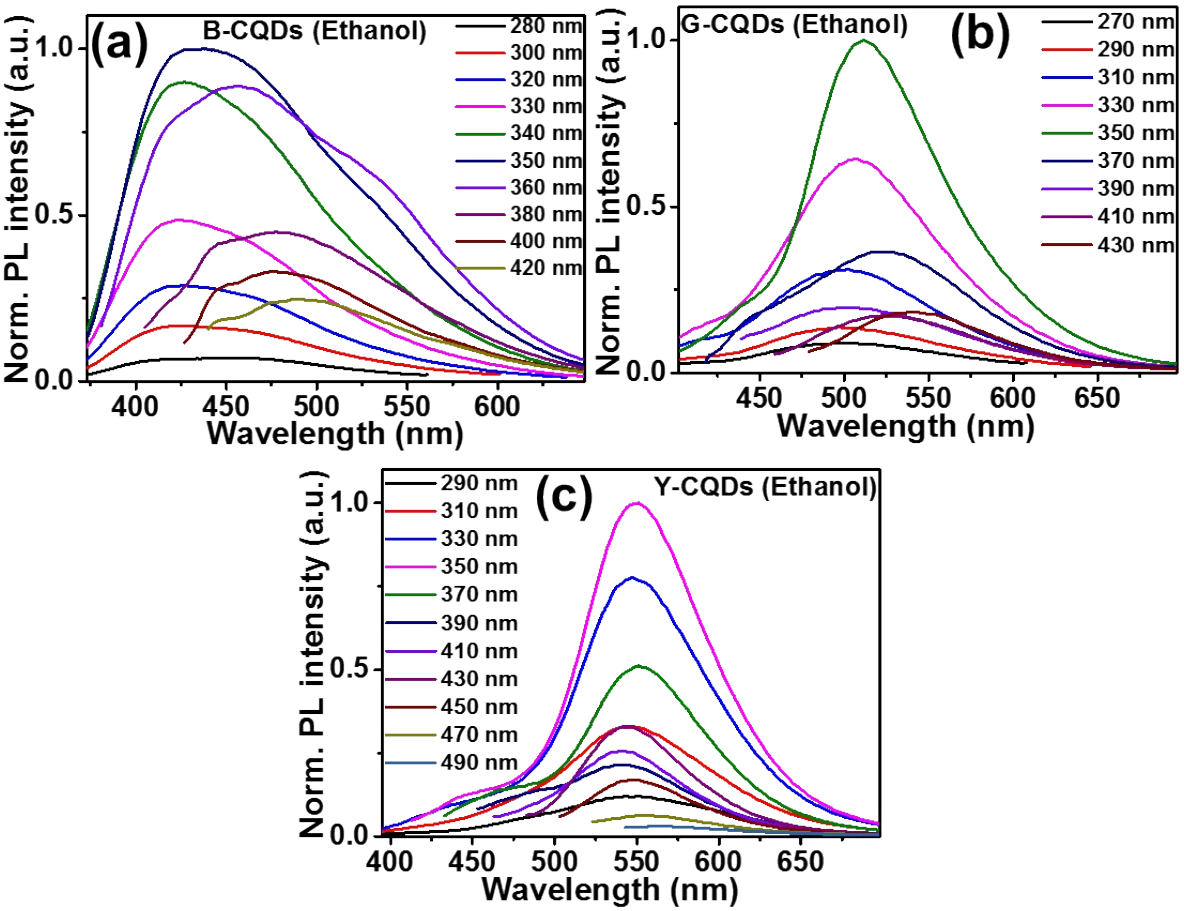

Fig. S3. PL emission spectra of (a) B-CQDs (b) G-CQDs and (c) Y-CQDs at different excitation wavelengths dispersed in ethanol.

Time-resolved fluorescence lifetime decay analysis

We also checked the time-resolved fluorescence lifetime decay analysis to get more understanding of the recombination dynamics. Fig. S4 shows the fluorescence decay profile, which is well fitted by the double exponential function according to the following equation:

$$R(t) = B_1 \, exp\left(\frac{-t}{\tau_1}\right) + B_2 \, exp\left(\frac{-t}{\tau_2}\right) \quad \text{.....(1)}$$

where R (t) is the sum of individual single exponential decays, B_1 and B_2 are the pre-exponential factors, τ_1 and τ_2 are the decay times. The average lifetime τ_{ave} of the CQDs Were calculated according to the following equation:

$$\tau_{ave} = \frac{B_1 \tau_1^2 + B_2 \tau_2^2}{B_1 \tau_1 + B_2 \tau_2} \quad \text{..... (2)}$$

The average lifetime (τ_{ave}) of B-, G-, and Y-CQDs were calculated to be 5.86, 7.3, and 6.88 ns which are well consistent with the QY data.

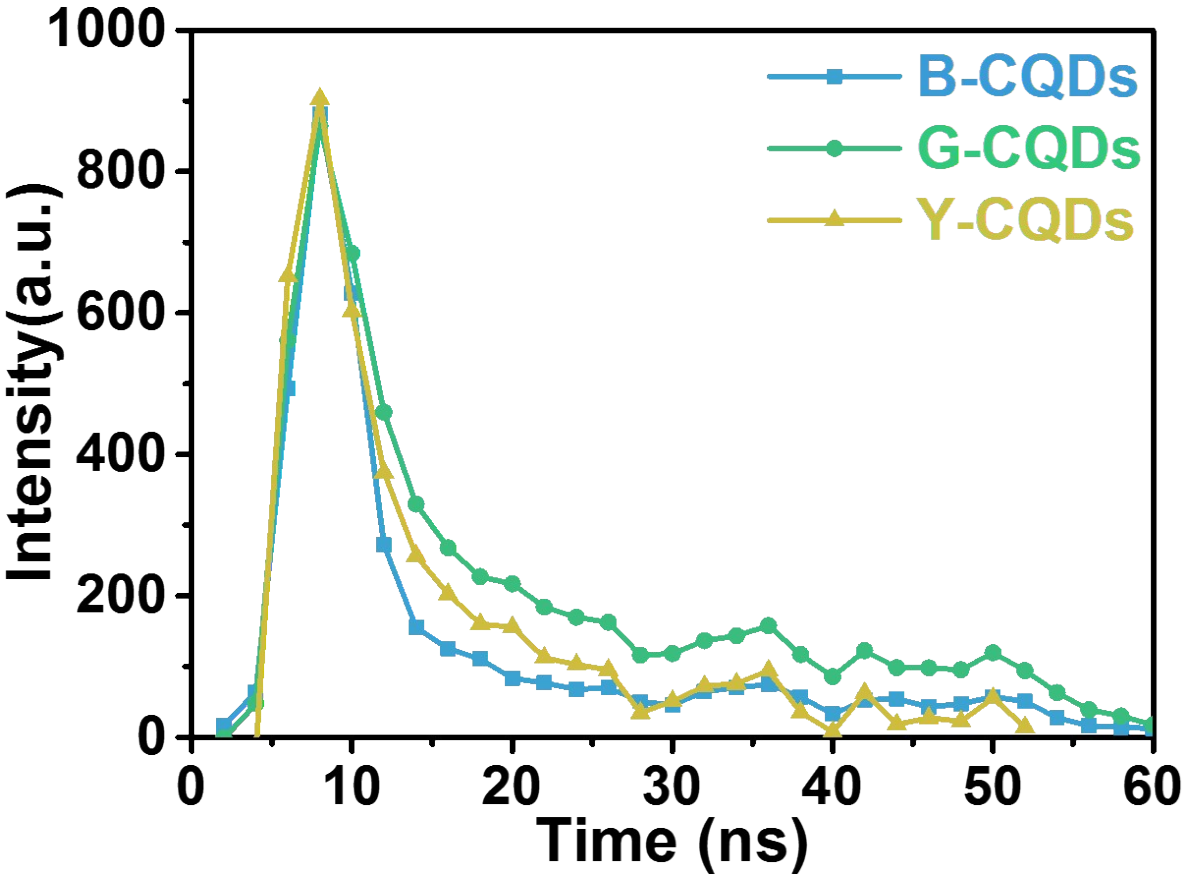

Fig. S4. Time-resolved fluorescence lifetime decay analysis

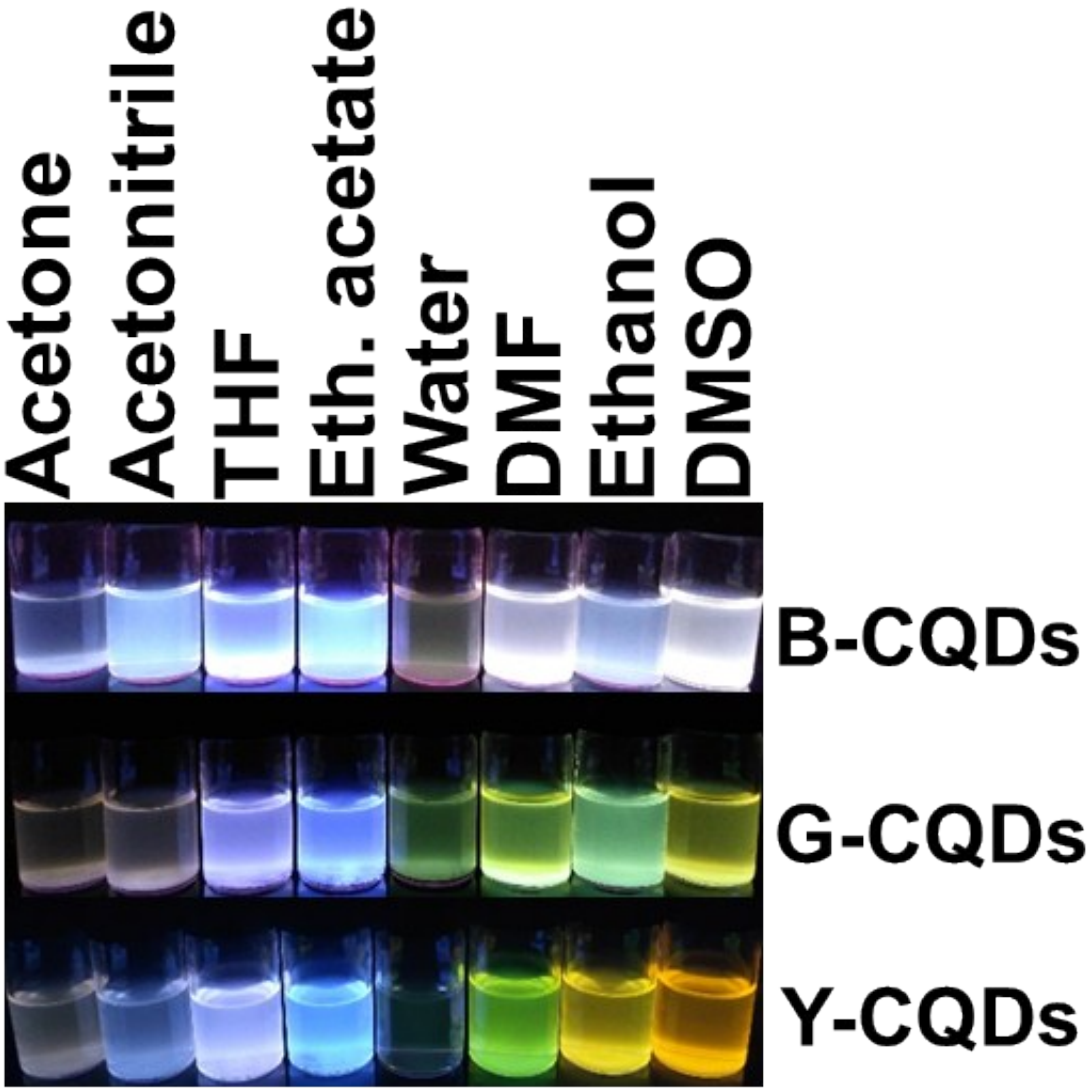

Fig. S5. Digital photographic image of fluorescence emission color of B-CQDs, G-CQDs, and Y-CQDs dispersed in various solvents of different polarity.

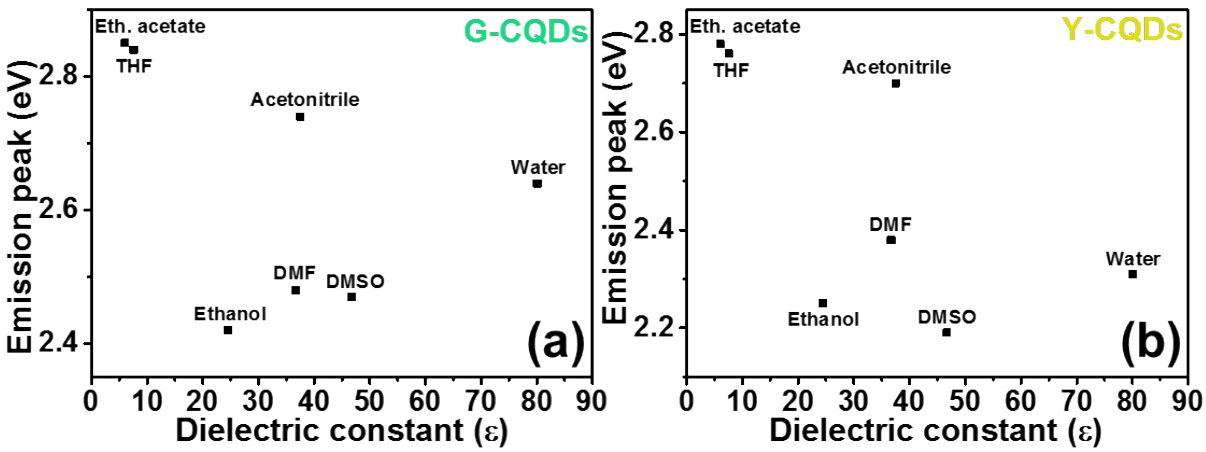

Fig. S6. Emission peak as a function of dielectric constants (ε) of solvents for (a) G-CQDs and (b) Y-CQDs

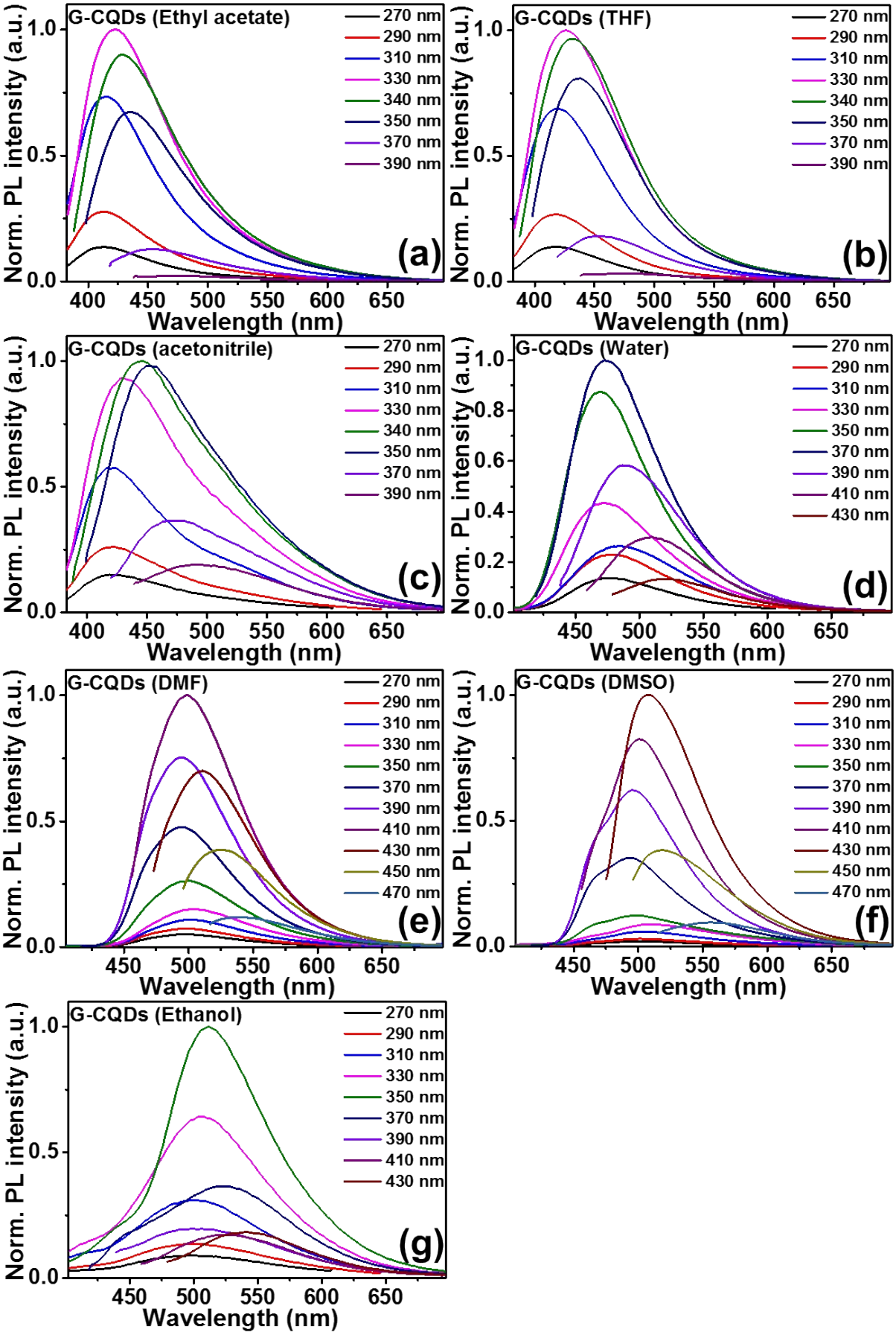
G-CQDs (Ethyl acetate)
(a)
G-CQDs (THF)
(b)
G-CQDs (acetonitrile)
(c)
G-CQDs (Water)
(d)
G-CQDs (DMF)
(e)
G-CQDs (DMSO)
(f)
G-CQDs (Ethanol)
(g)
Norm. PL intensity (a.u.)
Wavelength (nm)
270 nm
290 nm
310 nm
330 nm
340 nm
350 nm
370 nm
390 nm
410 nm
430 nm
450 nm
470 nm

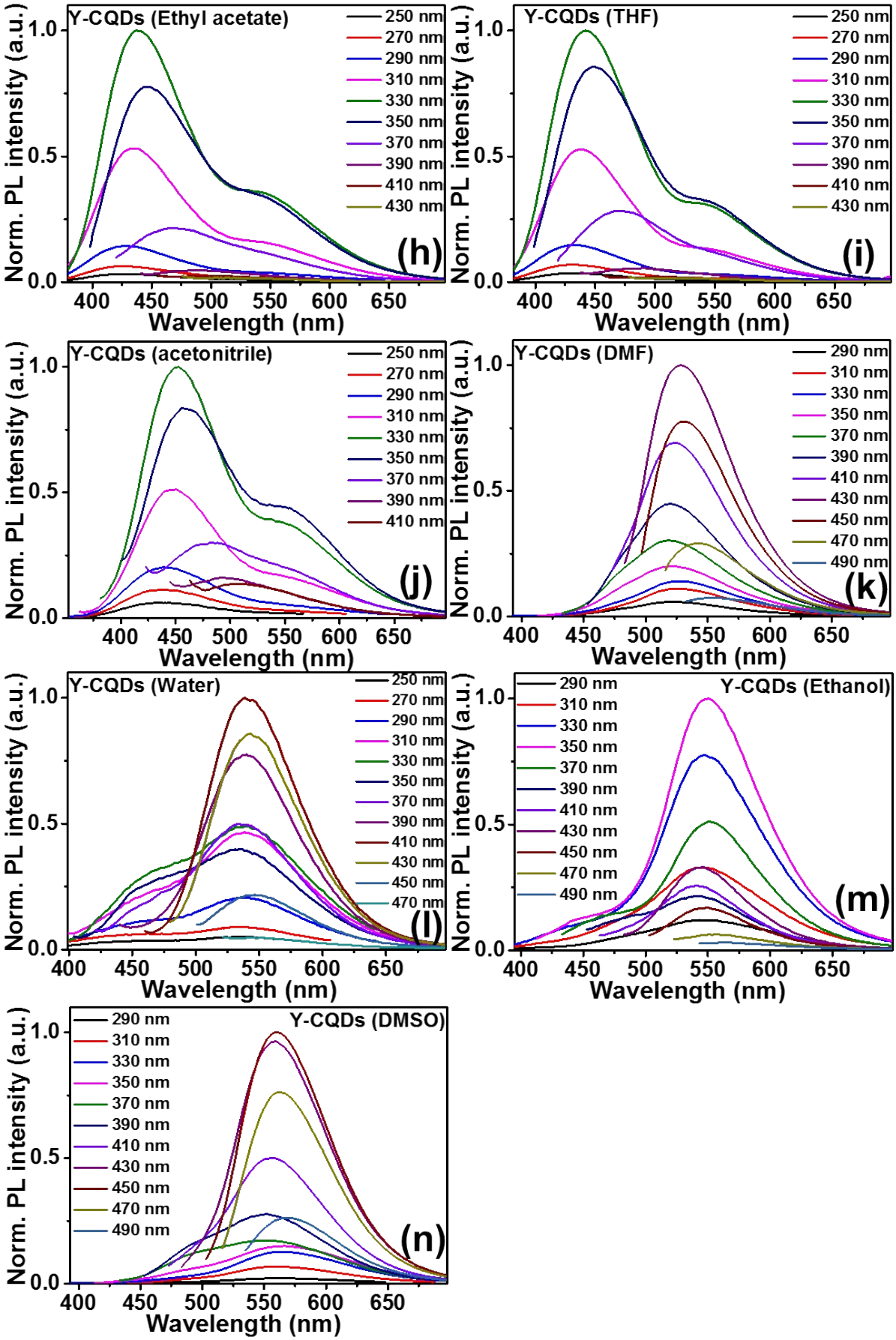
Y-CQDs (Ethyl acetate)
250 nm
270 nm
290 nm
310 nm
330 nm
350 nm
370 nm
390 nm
410 nm
430 nm
(h)
Norm. PL intensity (a.u.)
Wavelength (nm)
Y-CQDs (THF)
(i)
Y-CQDs (acetonitrile)
(j)
Y-CQDs (DMF)
290 nm
450 nm
470 nm
490 nm
(k)
Y-CQDs (Water)
(l)
Y-CQDs (Ethanol)
(m)
Y-CQDs (DMSO)
(n)

Fig. S7. PL emission spectra of G-CQDs (a, b, c, d, e, f, and g) and Y-CQDs (h, I, j, k, l, m, and n) at different excitation wavelengths dispersed in different polarity solvents (Ethyl acetate, THF, acetonitrile, DMF, water, Ethanol, DMSO)

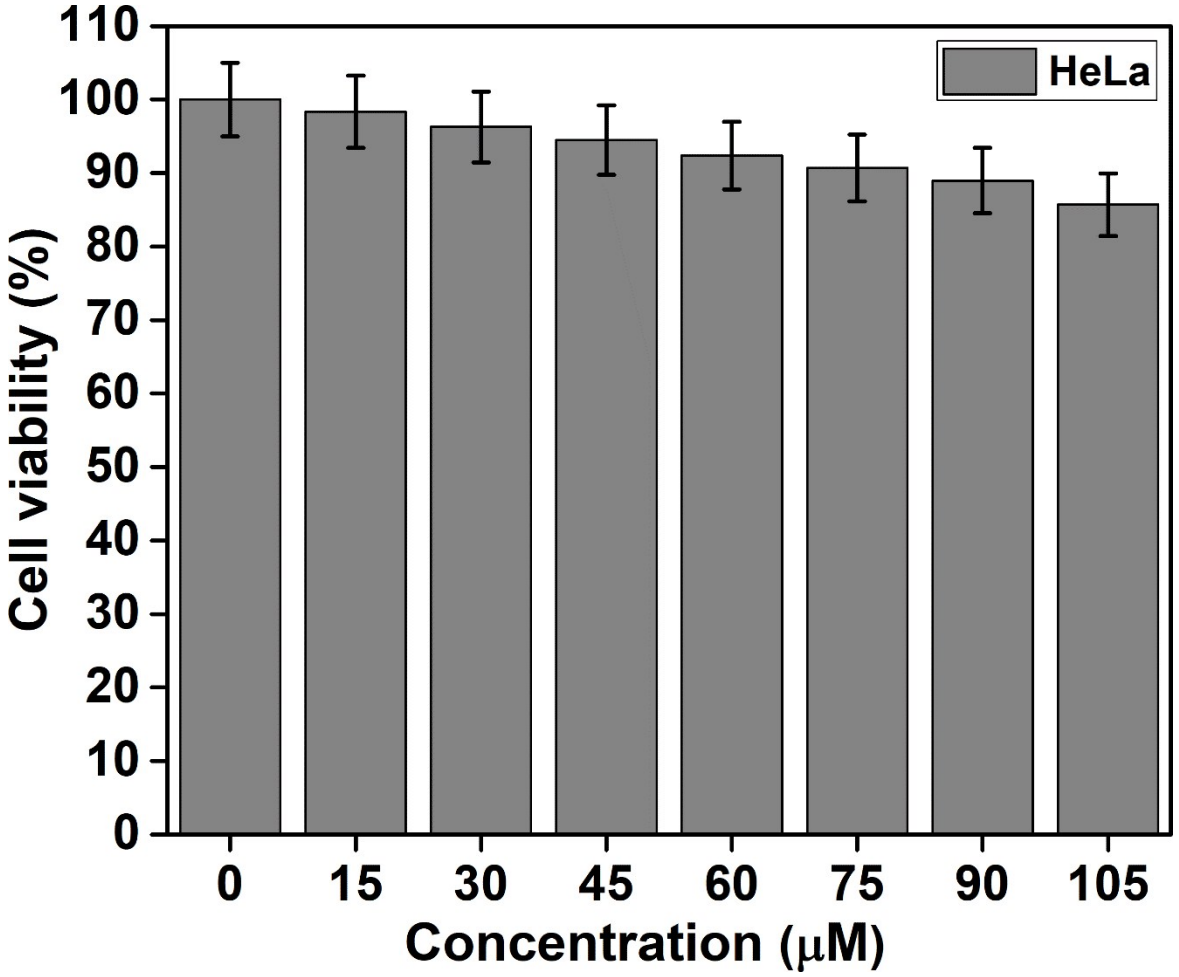

Fig. S8. Viability of HeLa cells after 24 h incubation with different concentration (0, 15, 30, 45, 60, 75, 90, and 105 μg/mL) of mixture of B-, G-, and Y- CQDs.

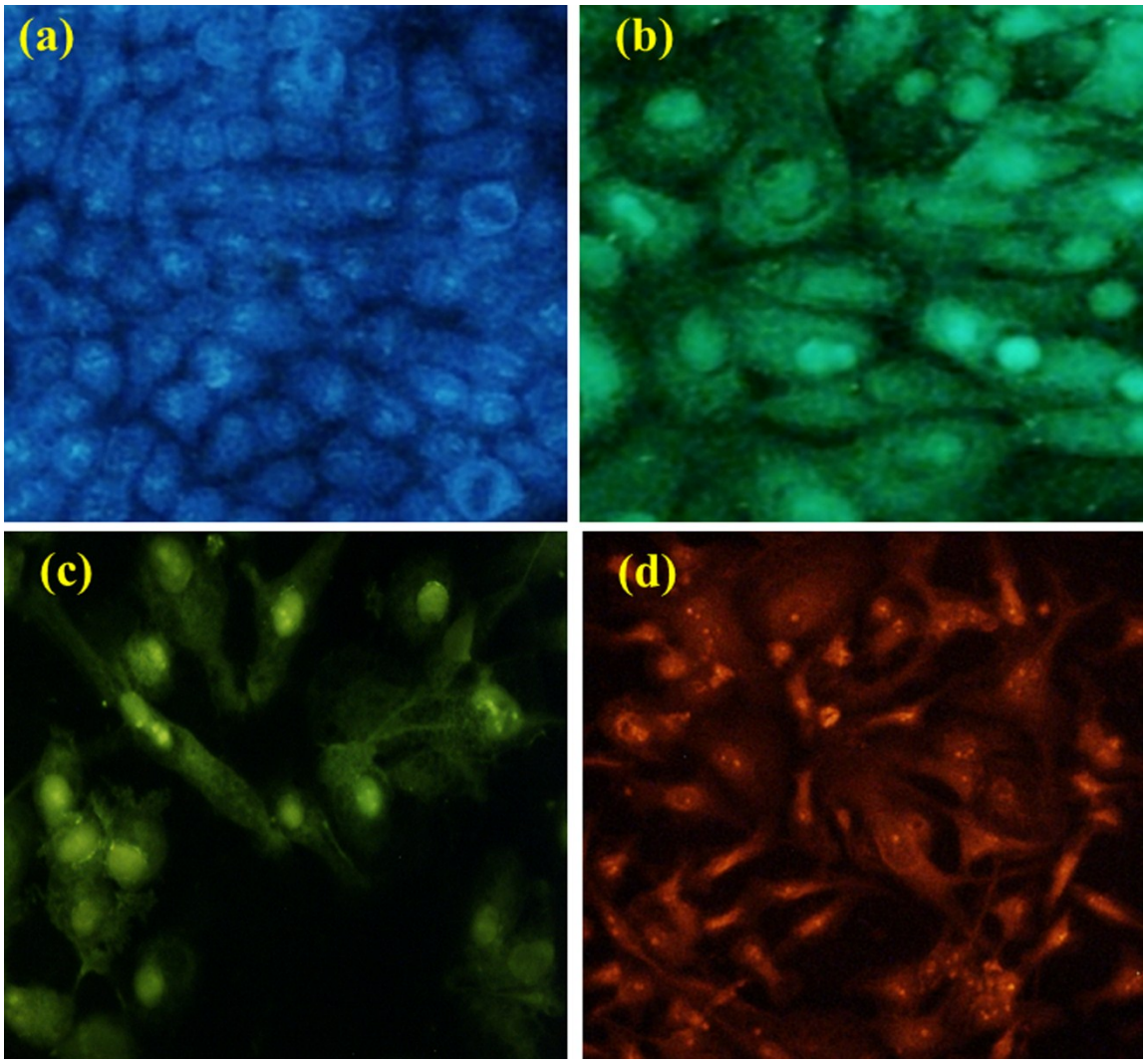

Fig. S9. High resolution fluorescence microscope images of HeLa cells incubated with (a) B-CQDs, (b) G-CQDs, and (c, d) Y-CQDs for 24 h. The four images were obtained under (a) 405 nm, (b) 441 nm (c) 488 nm and (d) 543 nm excitation.

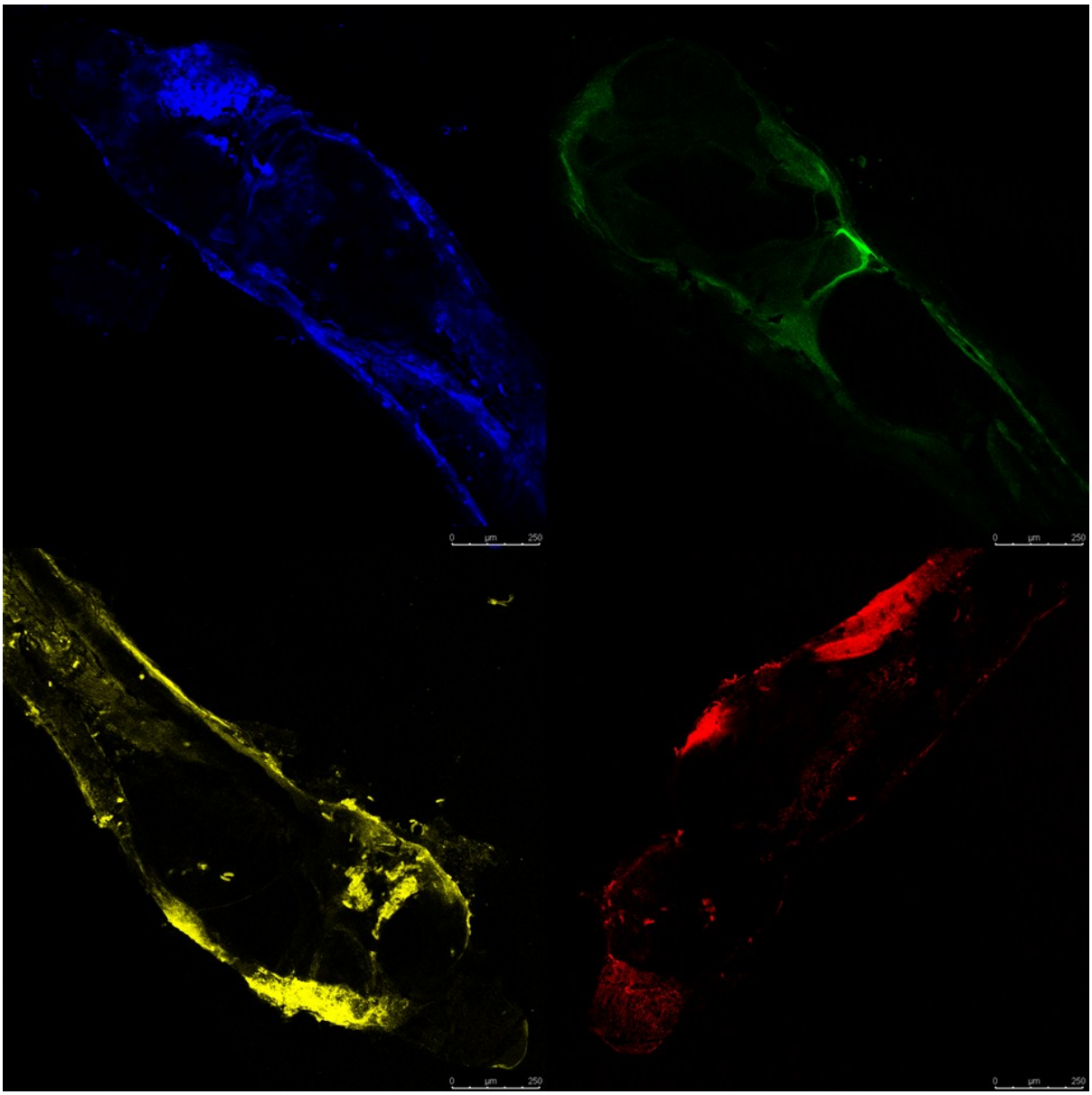

Fig. S10. Multicolor images of zebra fish larvae under confocal microscopy, with blue (B-CQDs), green (G-CQDs), yellow (Y-CQDs) and red (Y-CQDs) emissions

Table S1. comparison table of QY for different multicolor CQDs from literature

Materials	Synthesis method	QY				References
		Blue	Green	Yellow	Red	
citric acid and diaminonaphthalene	solvothermal	75	73	58	12	[5]
citric acid and urea	Thermal pyrolysis	52.6[+]	35.1	No	12.9	[7]
citric acid and urea	solvothermal	27.3	31.1	22.9	8.8	[8]
ammonium citrate and ethylenediamine tetraacetic acid	solvothermal	65.8	46.1	32.8	30.4	[9]
citric acid and urea	solvothermal	7.58-19.4	4.4-27.8	11-14.6	2	[12]
Candle soot and nitric acid	reflux	0.8	1.9	0.8	no	[15]
phloroglucinol	solvothermal	66	72	62	54	[20]
Manilkara zapota fruits.	Sonication and thermal heating	5.7	7.9	5.2	no	[29]
hydroquinone and ethylenediamine	hydrothermal	9.32	78.68	1.47	no	[57]
Phloroglucinol	Thermal heating in beaker	1.03	23	6.95	no	This work

Hydrothermal treatment

In this facile wet chemistry based synthesis method, it is very easy to track the product with specific fluorescence due to open system via monitoring the reaction time which is not possible in closed system (solvothermal in poly(tetrafluoroethylene)-lined autoclave). For better clarification, we performed the reaction in closed system (poly-tetrafluoroethylene-lined autoclave) keeping the reaction condition unaltered for 90 min in correspondence with Y-CQDs. Interestingly, we didn't get yellow emission (Y-CQDs) rather we only observed blue emissive CQDs with PL emission maxima λ_{em}= 440 nm. The digital photograph of fluorescence emission under UV-irradiation and the excitation-dependent PL emission spectra of the as-synthesized CQDs are detailed in Fig. S11 (ESI†). Thus, in view of the above experiment, it can be concluded that rapid synthesis of shape-specific CQDs are evidenced in open system thermal heating probably due to enhanced surface air-oxidation in presence of aerobic O_2 during the dehydration mediated controlled growth process. The related normalized excitation dependent PL emission spectra and the digital image under UV-irradiation is shown below.

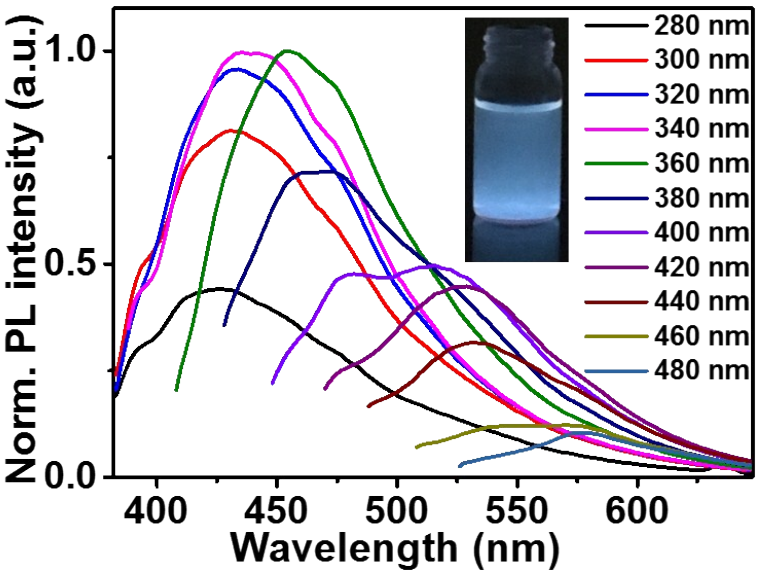

Fig. S11. Normalized excitation dependent PL emission spectra of hydrothermally treated phloroglucinol in closed system (poly-tetrafluoroethylene)-lined autoclave).